Egypt. J. Chem. **Vol. 67** No. 3 pp. 127 - 138 (2024)

Egyptian Journal of Chemistry

http://ejchem.journals.ekb.eg/

Preparation and Characterization of Nanocomposite Forward Osmosis Membranes for Water Desalination

Fatma Mohamed El-Sayed[a], Abo El-Fadl, M[a], Abo Aly M. M.[b], Heba Isawi[a] and Mohamed, E.A.Ali [a]

[a] Hydrogeochemistry Department- Desert Research Center.

[b] Chemistry Department- Faculty of Science, Ain Shams University.

Abstract

In this study, interfacial polymerization was used to synthesize a thin film–composite (TFC) membrane for forward osmosis (FO) applications; moreover, graphene oxide (GO) nanosheets (GONs), a dopamine solution (DA), and naturally accessible humic acid (HA) were synthesized on a polyethersulfone (PES) substrate. The effects of the different quantities of GO, HA, and DA on the membrane surfaces as well as their various cross-sectional morphologies and FO desalination capabilities were investigated. The integrated TFC membrane containing an appropriate blend of GO, HA, and DA outperformed the control membrane, obtaining high water flux, and high salt rejection. Furthermore, the chlorine resistance of the enhanced membrane was 75 times that of the control membrane.

Keywords: Forward Osmosis, GO Nano Sheets, Humic Acid, Dopamine,Thin Film Composite, and Desalination Performance.

1. Introduction

Desalination is the extraction of salts from seawater or brackish water to produce drinking water for humans and animals as well as clean water for irrigation and industrial purposes (**Marcovecchio *et al.* 2005**). The forward osmosis (FO) technology has recently piqued the interests of scholars and industries. This technology exploits the difference in the osmotic pressures of a low-concentration feed solution (FS) and a high-concentration draw solution (DS) to transport water molecules between semipermeable membranes (**Zhao *et al.* 2012**). The FO technology exhibits several advantages, such as reduced operating energy input **(Mazlan *et al.* 2016**), more efficient contaminant rejection **She *et al.* (2013) and Kong *et al.* (2014)** and reduced possibility of membrane fouling, compared with reverse osmosis **Emadzadeh *et al.* (2014) and Salehi *et al.* (2017).**

Consequently, increased efforts have been invested in recent years to optimize and improve the permeability–selectivity of membranes. An increased water permeability at constant salt rejection or decreased salt permeability at constant water permeability could increase the permeability selectivity (**Werber *et al.* 2016**). A previous study demonstrated that a substrate with a large pore size benefited the synthesis of thinner polyamide (PA) layers. Thus, several hydrophilic materials, such as sulfonated polyphenylene sulfone, have been developed (**Singh *et al.* 2006**), and graphene oxide nanosheet (GO)(**Ghosh and Hoek. 2009**) and (**Widjojo *et al.* 2013**), carbon nanotubes (**Liu *et al.* 2016**) and (**Obaid *et al.* 2018**), titanium dioxide nanoparticles, etc., have been added to the substrate. By incorporating hydrophilic elements into the substrate and enhancing its porous structure, the water resistance of such substrates can be enhanced (**Shaffer *et al.* 2015**) and (**Song *et al.* 2016**).

GO was added during the formulation of the ultrafiltration PES membrane to increase the water flux of the membrane (**Ma *et al.* 2017**). These GO membranes increased the thermal stability and mechanical qualities of the PES membranes. For the interfacial polymerization (IP) of PA, a PES–GO-based substrate was studied (**Park *et al.* 2015**). Thin

*Corresponding author e-mail: afr_2017sc@yahoo.com.; (Fatma Mohamed El-Sayed).

Receive Date: 18 July 2023 Revise Date: 17 September 2023 Accept Date: 03 October 2023

DOI: 10.21608/EJCHEM.2023.223871.8279

film–composite (TFC) FO membranes were layered. Moreover, a previous study confirmed that the incorporation of GO into membranes can improve their water permeability. Furthermore, in a previous study (**Ali *et al.* 2016**), FO membranes were synthesized by adding only 76 ppm GO to the aqueous phase during IP.

Humic compounds contain carbon polymers with oxygen-containing functional groups, e.g., hydroxyl, carboxylic acid, ketone, and quinone groups, that are naturally available **Huang *et al.* (2018) and Zhou *et al.* (2018)**. Moreover, humic acid (HA), which is a macromolecular material, exhibits a high dispersion capacity. Additionally, HA is an environment-friendly material (**Jing *et al.* 2014**). A previous study (**Guan *et al.* 2017**) revealed that HA can improve the pore-size distribution of PES membranes, thereby increasing their pure water permeability. Moreover, studies have shown that the introduction of HA into GO enhances the molecular diffusivity of water and the permeability of the GO membrane (**Konch *et al.* 2018**).

Furthermore, the chemistry of dopamine (DA) or polydopamine (PDA) offers a new path for producing high-performance membranes. In a previous study (**Xi *et al.* 2009**), a novel method was designed for performing surface modifications using DA and polyethylene (PE) to considerably enhance the permeability of the membranes. Using the IP technique, single DA in an aqueous solution successfully enhanced the structural and chemical stabilities of the membrane (**Zhao *et al.* 2014**). In a previous study **Huang *et al.* (2015) and Han *et al.* (2012).** TFC–FO membranes were prepared on the top surface of PDA-modified PES substrates; the thickness of the PA layer decreased with increasing salt rejection on the membrane substrates at a short PDA-coating time.

A previous study (**Xu *et al.* 2017**) reported that the constructed novel membrane exhibited improved water flux after the addition of DA into a 1,3-metaphenylenediamine (MPD) solution, although it exhibited increased reverse salt flux and PA-layer thickness. The thickness of the layer increased compared with that of the control membrane. Thus, the impact of different DA concentrations of the aqueous phase that was paired with MPD on the properties and performance of the FO membrane must be investigated.

Fertilizers are anyway extensively used in the agricultural production and, their use will continue to rise to feed the growing world population. In such a situation, fertilizers can be used as draw agents for FO process because the diluted draw solution can be directly applied for fertigation. This concept offers several novelties: firstly the cost of desalinated water remains very low, secondly draw solution need not undergo an additional separation process and thirdly the process provides nutrient rich water for irrigation of plants and crops. Besides, FO desalination has high recovery rate and high salt rejection rate **McCutcheon *et al.* (2005) and Cath *et al.* (2006)** which will be an additional advantage for the irrigation application.

In this study, different concentrations of GO and HA were added to a PES substrate and different concentrations of DA were added into MPD to improve the permeability–selectivity properties of a TFC–FO membrane. Further, the best concentrations of GO, HA and DA were compared. Thereafter, membranes were synthesized by combining GO, HA and DA. Thus, this study revealed an effective and ecologically acceptable substance that could be doped into the TFC–FO membrane substrate to alter the physicochemical properties of the membrane and improve its permeability–selectivity characteristics.

2. Experimental

2.1. Materials

Polyethersulphone (PES), Polyvinylpyrrolidone (PVP), hexane, and 1, 3, 5-benzenetricarbonyl trichloride (TMC) with a virtue of >98% scattered in hexane (98%) were provided by Sigma–Aldrich. Also, N, N-dimethylacetamide (DMA) and 1, 3-phenylenediamine were purchased from Sigma–Aldrich. Also, Analysts have utilized graphite; $NaNO_3$, H_2O_2, H_2SO_4, and $KMnO_4$ were purchased from Sigma–Aldrich to prepare GO nanosheets (GONs). While HA and DA was bought from Biodiagnostic. For the FO explore, sodium chloride (NaCl) was dissolved in deionized water (DI). Sodium alginate, (KH_2PO_4), magnesium chloride ($MgCl_2$), sodium hydrogen carbonate ($NaHCO_3$), calcium chloride ($CaCl_2$), and ammonium chloride (NH_4Cl) (El Gomhouria Company) were utilized for the layer fouling tests.

2.2. Methods

2.2.1 Preparation of GONs

GONs were synthesized using graphite powders via the classical Hummer method **Hummers and Offeman (1958); Hirata *et al.* (2004)** & **Park and Ruoff (2009).** Briefly, 1.0 g of graphite and 0.5 g of $NaNO_3$ were added into a flask containing 23.0 mL of a concentrated H_2SO_4 solution and stirred in a cold water bath. Subsequently, 3.0 g of $KMnO_4$ was added gradually for 2.0 h before the mixture was transferred to a 35.0°C water bath and stirred for 0.5 h. Thereafter, 46.0 mL of DI water was added gradually, and the reaction mixture was kept at 98.0°C for 0.5 h. Finally, 140.0 mL of DI water was added to the mixture and stirred. The resulting mixture was heated for 1 h at 95°C without allowing it to boil. Then, the heater was switched off, and the reaction mixture was allowed to cool by adding 500 mL of DI water with stirring for 1 h. Next, 40.0 mL of an H_2O_2 solution was added to the mixture to terminate the reaction. To obtain the final product,

the mixture was filtered and rinsed three times with DI water; after which, the as-prepared GONs were washed three times with DI and methanol, successively, to remove the residues. Finally, the powders were baked at 60°C for 12 h.

2.2.2 Preparation of Polyethersulfone (PES) Substrate

To prepare the casting solution using PES, a mixed solvent system containing PVP (5 g) and DMA (75 g) was prepared by ultrasonicating the system for 10 min, and different concentrations of HA (0.1, 0.3, 0.5, 0.8, and 1 wt.%) and GO (0.1, 0.25, 0.5, 1, and 1.5 wt.%) were added. Each compound was added to the solution and ultasonicated for 30 min at room temperature. Thereafter, the solutions were added with stirring for 30 min. Subsequently, 25 g of PES was added into the solution with stirring for 24 h and placed on a stand where it was kept overnight. Then, the solution was placed on a glass plate and distributed onto the films. After 30 min, the membranes were stored in a DI water bath at 4°C.

2.2.3 Preparation of thin film composite (TFC) membranes

The TFC membranes were prepared via IP using the mixed amine (MPD and DA) solution and TMC at the surface of the PES substrates. Specifically, the TFC membranes were prepared by blending 2.0 wt.% of MPD and certain concentrations of DA (0.0, 0.01, 0.05, 0.3, 0.5, and 0.8 wt.%). The PES substrate was immersed in the prepared solution for 30 min to ensure the complete soaking and adequate self-polymerization of DA (PDA). Thereafter, the substrate was dipped in a TMC solution (0.15 wt.% in hexane) for 1 min to initiate IP. Subsequently, the substrate was removed from the hexane natural section and set vertically for 2 min to evaporate the residual solution. Afterward, the as-prepared substrate was vacuum dried at 70°C for 5 min. Finally, the obtained composite membranes were washed and stored in DI water (4°C) for the subsequent experiments.

2.3 Characterizations of synthesized membranes

The membranes are characterized by each following XRD SEM, and the contact angle. X-ray diffraction (XRD) data were recorded on 2nd Gen D_2 – PHASER BRUKER. The scanning electron microscope (SEM Quanta FEG) was used to characterize the membrane surface and cross-section characteristics. The contact angle was utilized to estimate the membrane hydrophilicity by a Cam-positive Micro, Tantec Inc. pattern. A water droplet was located onto the membrane surface after air-dried at 25°C utilizing DI water by a numerical micro-syringe. The contact angle testified with an average of five measurements were obtained for each membrane sample on different locations.

2.3.1 XRD analysis

XRD Analysis to determine composition of the PES/TFC, PES/TFC+DA, PES+GO/TFC, PES+HA/TFC and (GO+HA+DA)/TFC membranes. **Fig (1)** shows the XRD spectrum of PES/ TFC, DA/ TFC, GO/ TFC, HA/ TFC and (GO + HA+ DA) /TFC membranes. As can be seen, the PES polymer shows a peak at 2θ = 17.5°, which is similar to the reported peak of (**Khayet and García 2009**).

Also, it can be seen, the humic acid shows a peak at 2θ = 16.5°, 21.5, 24°, 41° and 48°, which is similar to the reported peak by (**Santos *et al.* 2018**). Where, according to (**Luo *et al.* 2015**). The dopamine shows peaks at 2θ =17.5°, 22°, 25°, 42° and 49°. The peaks appear at 2θ= 41°, 42° and 48° related to the modification of the TFC membrane with Graphene oxide Nanosheet (**Siburian *et al.* 2018**).

It observed that the count of peaks increases at the modification of the TFC membrane especially with the (GO+ HA+DA) mixture. Also, there are disappearing peaks such as the peak at 2θ= 45º. Therefore, the modification of the TFC membrane with (GO+ HA+DA) mixture gives the best results due to this membrane containing the characteristics of three materials (GONS, DA and HA). The oxygenated functional groups—such as hydroxyl, epoxy and carboxyl—on its basal plane and at its edge. (**Lerf *et al*. 1998**). Also, these functional groups endow GO good hydrophilicity and favorable water solubility, which enables a convenient and cost-effective solution process for the preparation of membrane. This lead to a drastic increase in permeates fluxes **(Szabó *et al.* (2005)** and **Huang *et al.* (2013)**.

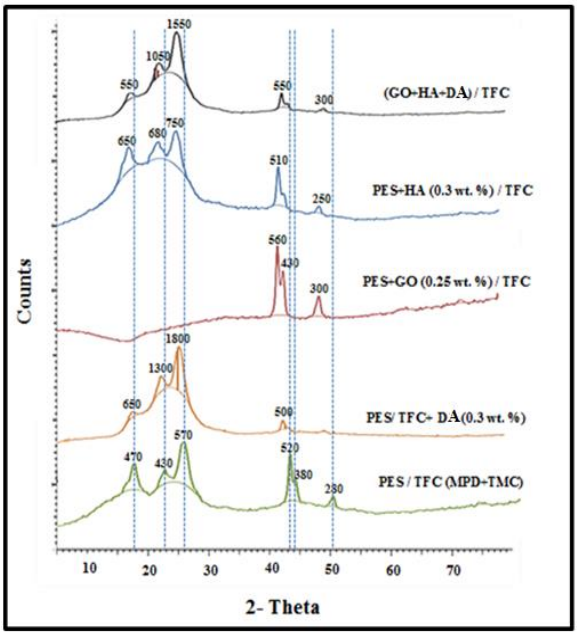

Polyethersulfone (PES), humic acid (HA), Graphene oxide (GO), thin film composite (TFC), 1, 3-phenylenediamine (MPD), 1, 3, 5-benzenetricarbonyle trichloride (TMC) and dopamine (DA).

Fig. (1). PES/TFC+DA, PES+GO/TFC, PES X-ray diffraction patterns of PES/TFC, +HA/TFC and (GO+HA+DA)/TFC membranes.

2.3.2 Contact angle of FO membranes

The contact angles of the control; DA/TFC; GO/TFC; HA/TFC; and HA, GO, DA/TFC–modified membranes are shown in **Fig. (2).** The contact angle is the greatest collective factor utilized to define the hydrophilicity/ hydrophobicity of membrane surfaces. Generally, a small contact angle ($0° < \theta < 90°$) corresponds to the high hydrophilicity of the membrane, while a high contact angle ($90° < \theta < 180°$) corresponds to its high hydrophobicity.

Figure (2) shows that the average contact angles of the control; HA/TFC; GO/TFC; DA/TFC; and HA, GO, DA/TFC–modified membranes are 69° ± 2°, 53.6° ± 1.2°, 57° ± 1.2°, 64.3° ± 1.6° and 35.9° ± 6°, respectively, demonstrating that the membranes exhibit hydrophilic surfaces. The presence of the OH and COOH groups causes the high hydrophilicity of the membrane. The DA/TFC-modified membrane exhibited a lower contact angle of ~64° at 25°C, signifying that its hydrophilic surfaces improved with the incorporation of DA into the polymer casting mixture. The increased hydrophilicity of the DA-modified TFC membrane could be attributed to the stronger attraction of the H_2O molecules by DA.

The contact angle decreased after the addition of DA, increasing the surface energy of the membrane. This can allow an easy movement of H_2O over the surface of the membrane to enhance the capacity of the hydrophilic pores to absorb H_2O through their capillary properties. When 0.25 wt. of GO/TFC membrane was added, the contact angle decreased to 57°, increasing the hydrophilicity of the membrane via the incorporation of GO mainly as a pore-generating agent. Moreover, the contact angle was further reduced to 53° after the incorporation of HA in the TFC membrane. These results corroborated with the results of previous research on improving the hydrophilicity of PES and TFC films via the incorporation of GO and HA **Ghaseminezhad *et al.* (2019).** The incorporation of hydrophilic GO and HA slightly increased the hydrophilization of the membrane, as observed by a decrease in the contact angle. Further, the incorporation of the hydroxyl, carboxylate and epoxy moieties would enhance the hydrophilicity of the HA, GO, and DA/TFC–modified membrane.

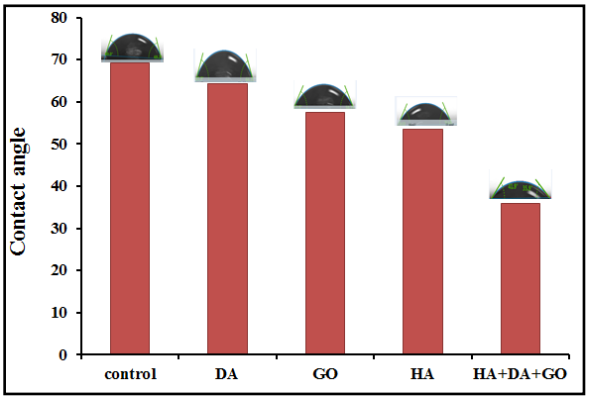

Fig. (2). the water contact angle control, DA/TFC, GO/TFC, HA/TFC and HA+DA+GO/ TFC modified membranes surfaces.

2.3.3 Analysis of the morphology of the membranes

A scanning electron microscope (SEM) analysis was performed to examine the forms and dispersions of HA, DA, and GONs within the composite membranes. The surface structures of PES, PES+GO, PES+HA, PES+GO+HA, PES+TFC, PES(GO+HA)+TFC and PES(GO+HA)+(TFC+DA) membranes are shown in the SEM images **Figs.(3a-g))**. Additionally, **Fig. (3 h &i)** shows the surface structure of the GONs. The morphologies of the HA and DA membranes confirm the increase in the size and number of pores on the surface of the membranes.

Figure 4 (a-g) show the cross-sectional SEM images of PES, PES+GO, PES+HA, PES+GO+HA, PES+TFC, PES(GO+HA)+TFC and PES(GO+HA)+(TFC+DA) membranes, respectively. The as-prepared membranes exhibited an asymmetric structure comprising a porous support/sublayer with cellular morphologies and a thin dense skin layer. The membranes exhibited straight finger-like microvoids, which expanded and were bent toward the center and further elongated until they reached the bottom of the membrane, upon GO, HA, and DA incorporations. Further, the cellular pores were broadened and the thin walls interacted. The microvoid structures of the composite GO, HA, and DA membranes expanded and the number of pores increased after the addition of the hydrophilic materials owing to the instantaneous demixing of the membrane material in the solvent. Further, the thin layer of the composite PES membranes became thinner than that of the control PES membrane. The transportation of water molecules across the membrane via narrow interspaces significantly enhanced it. In addition to improving the permeation flux, a highly hydrophilic membrane could also minimize fouling of the membrane surface (**Chang *et al.* 2014**).

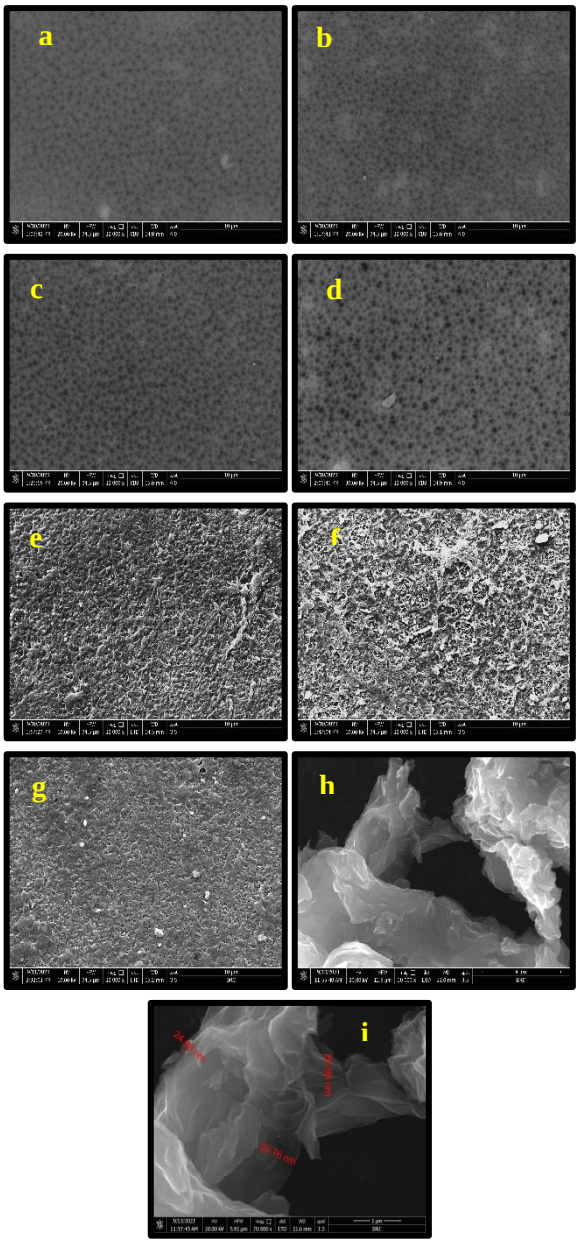

Fig. (3). SEM images surface for a) PES, b) PES+GO, c) PES+HA, d) PES+GO+HA, e) PES+TFC, f) PES(GO+HA)+TFC , g) PES(GO+HA)+(TFC+DA), and h, i) GONs .

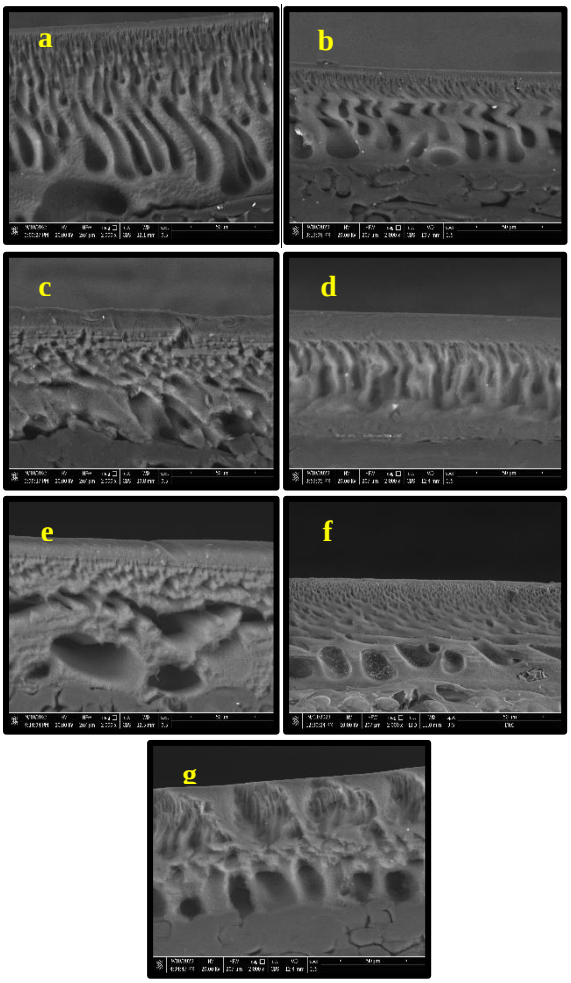

Fig. (4). SEM image cross sections for a) PES, b) PES + GO, c) PES + HA, d) PES + GO + HA, e) PES + TFC, f) PES (GO + HA) + TFC and g) PES (GO + HA) + (TFC + DA).

2.3.4 FO performance tests

The FO membrane comprising a strong membrane (42 cm^2) was utilized. Two variable speed gear pumps were used to circulate the feed and draw solutions concurrently. Flow rates of the feed and draw solutions were monitored with Rota meters. The temperatures of the feed and draw solutions were set at 25°C. The membranes were examined in the FO mode (i.e., the active layer (AL) was passed through the feed solution (FS)). To compare the overall FO performance of the thin-film membranes, 2 M of NaCl and DI water were used as the DS and FS, respectively. The concentration of the salt extracted from the DS was measured. An electronic balance connected to a computer was used to record the mass of permeated water (m) into the draw solution. FO was allowed to proceed for ~2 h to ensure precise measurements. The obtained values were averaged from the calculated data that were collected after 10 min of operation. The FO flux (J_w, $Lm^{-2}h^{-1}$) was calculated using the Eq. below, where Q is quantity

of permeate collected in "L", A is the effective membrane surface area in "m^2" and Δt is sampling time.

$$\boldsymbol{Jw} = \frac{Q}{A\,\Delta t}$$

The salt rejection that was retained by membrane (R, %) was calculated as below

$$\boldsymbol{R}\% = \left(1 - \frac{Cd * Vd}{Cf * Vf}\right) * 100$$

Where C_d is the salt concentration in the draw solution after a given time, which was determined via standard curve method using a conductivity meter and V_d is the volume of the draw solution. C_f and V_f are the initial concentration and volume of the feed solution, respectively.

2.3.5 Evaluation of antiorganic fouling performance

The antifouling performance of the FO membrane was evaluated by adopting sodium alginate as module pollutant. The feed solution was composed of 250 mg L^{-1} sodium alginate, 0.45 mM KH_2PO_4, 9.2 mM NaCl, 0.61 mM $MgCl_2$, 0.5 mM $NaHCO_3$, 0.5 mM $CaCl_2$ and 0.93 mM NH_4Cl **(Lu *et al.* 2016).** In addition, 2 M of NaCl was used as the DS. The change in the cumulative volume of the DS was recorded every 10 min. The complete antifouling assessment experiment lasted for 600 min.

2.3.6 Evaluation of the chlorine resistance and overall performance of the membrane

The chlorine resistance of the examined membranes was evaluated by exposing their top surfaces to a NaClO solution (1000 ppm) for a given period. The NaClO solutions were stored in dark, and their concentrations were changed every 2h during the observation to maintain a consistent concentration. To quantitatively assess the chlorine resistance of the as-prepared membranes, a reduced loss of water flux indicated the drastic degradation of the PA layers. Owing to the vividness of chlorine, FO methods are no longer acceptable **Lu *et al.*** (**2018**) and **Wang *et al.* (2018**). Before the membrane FO performance tests, these membranes were removed from NaClO solutions and then washed 3 times with DI water to avoid the residual chlorine oxidation during tests.

3. Results and discussions

3.1 Desalination performance of the membrane

3.1.1 Optimum conditions of TFC control

Figure (5). Shows the water fluxes of the FO membranes when different doses of MPD (0.5, 1, 2 and 3 g/100 mL) and TMC (0.05, 0.1, 0.15 and 0.2 g/100 mL) were used. Additionally, different times for preparing MPD (1, 2 and 3 min) and TMC (0.5, 1 and 2 min) as well as different membrane thicknesses (30, 35 and 40 µ) were exploited to obtain the optimum condition for preparing the control membrane. The DS and FS modes used 2.0 M of NaCl and DI water as the DS and FS, respectively. The water flows of the optimum TFC membrane were recorded at 2 g/100 mL MPD; the TMC concentration was 0.15 g/100 mL and the MPD and TMC preparation times were 2 and 1 min. respectively**.** These optimum conditions are due to the increased pore size of the membrane and prevent accumulation which leads to a decrease in the efficiency of the membrane.

Understanding the mechanism of PA generation via interfacial polymerization is necessary to explain the observed patterns in **Fig. (5a & b).** When the MPD/water-impregnated PES support comes into contact with the TMC/organic solvent solution, the reaction starts at the surface. As a result of the immiscibility of water and organic solvents, the polymerization reaction takes place at this interface. Due to its low solubility, the MPD concentration in water is typically significantly higher than the TMC concentration in the organic solvent in reactions. Since the polymer film grows from the water/organic interface toward the bulk of the organic solution, it is thought that the reaction is primarily regulated by the diffusion of MPD molecules to the reaction zone.

The water/organic concept of universal is an empty platform for the rapid reaction of MPD and TMC molecules to generate an ultrathin incipient (core) PA film at the PES surface right after the two monomer solutions come into contact. When the incipient (core) layer is present, polymerization then changes to a slow growth stage, where the MPD diffusion and consequently the reaction rate drastically slow down. The creation of a second layer covering the core layer with the so-called ridge-and-valley shape is the result of polymerization at this stage. The final PA layer's ability to separate depends not only on the overall film thickness (the lower the water permeation, the thicker the film is) but also on the internal structure's crosslink density. A thicker PA layer with a larger ridge-and-valley structure forms at the surface because of the increase in the amount of MPD molecules that are available in the reaction zone, which encourages polymerization and raises the membrane's internal barrier to water flow **(Khorshidi *et al.* 2015).**

The observed trend for the influence of the TMC concentration was also confirmed by comparing the water flux of confirmation membranes in **Fig. (5c & d).** The incipient PA layer became sufficiently dense at higher TMC concentrations to prevent MPD molecules from diffusing to the organic phase and forming a thick ridge-and-valley structure during the reaction. This was caused by the presence of a greater number of TMC molecules in the reaction zone. There are two potential reasons for such a significant increase in water flux when the TMC concentration is raised:

first, the PA active layer's thickness may have decreased, which lowers the membrane's barrier to mass transfer and ultimately raises the water flux. Second, compared to thicker active layers, thinner active layers are more susceptible to being affected by subsurface morphology (such as support porosity and roughness). According to the reaction mechanism, extending the reaction time should result in a thicker film and, consequently, a membrane that is more resistant to water flow. Also, **Fig. (5 e)** shows that water flux decreases as TFC membrane thickness increases due to higher membrane resistance and lower membrane efficiency **(Ghosh and Hoek 2009).**

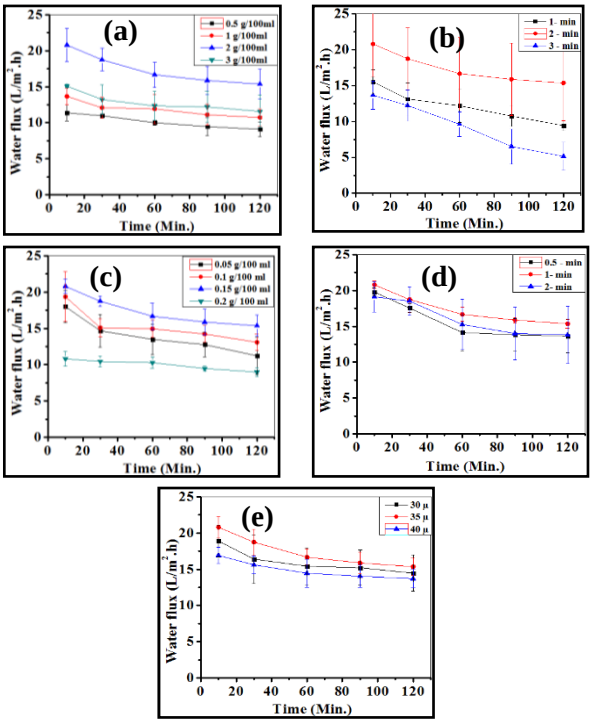

Fig.(5) Water fluxes of the TFC membranes in the AL-FS mode: (a) different concentrations of MPD (0.5, 1, 2 and 3 g/100 mL), (b) different preparation times of MPD (1, 2 and 3 min), (c) different concentration of TMC (0.05, 0.1, 0.15 and 0.2 g/100 mL), (d) different preparation times of TMC (0.5, 1 and 2 min) and (e) different thicknesses of the membrane (30, 35 and 40 µ).

3.1.2 Effect of different concentration of humic acid

The pure water permeability of the TFC membrane is shown in **Fig. (6).** Compared with the control membrane substrate, the HA-modified membrane substrate essentially exhibited pure water flux. The use of 0.3 wt.% of HA yielded the best result. The water flux increased to ~27.26 L/m^2.h, while the salt rejection reached 82%. This result is consistent with the results that large macrovoids, which increased the hydrophilicity of the membrane, were formed after HA doping. Based on these observations, we believe that the addition of HA to the mixture reduced the hydrophilic resistance and improved the permeability of the substrate. Further, the addition of more COOH functional groups to the PA layer afforded a more hydrophilic surface (**Guan *et al.* 2019**). The porosity initially increased with increasing HA amount from 0.1 to 0.3%wt. but decreased when its concentration was further increased to 1.0%wt. This "down-up" phenomenon was associated with the de-mixing of casting solution once the viscosity exceeded a certain value. The optimal HA concentration was found to be 0.3%wt. and the average pore radius of the fabricated membrane was lower than those at other dosages (0.1, 0.5, 0.8, and 1.0%wt.).

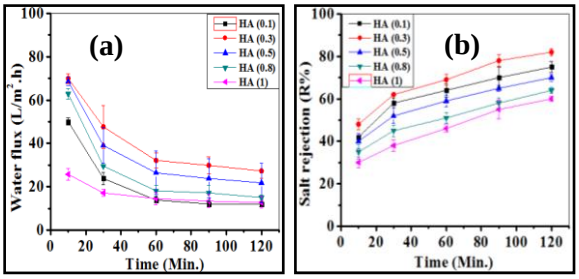

Fig. (6). (a) Pure water flux, (b) salt rejection of TFC with different concentrations of HA from 0.1 to 1 wt%.

3.1.3 Effect of different concentrations of GONs

Figure (7) presents the water flows of the FO membranes that were doped with different concentrations of GONs using 2.0 M of NaCl as the DS. As the concentration of GONs increased, the water fluxes increased initially before eventually reaching an ideal concentration value (0.25 wt.%). Thus, the ideal concentration of GONs was set at 0.25 wt.%. The water flux increased by ~16.43 L/m^2.h, while the salt rejection reached 89%, probably because of the improvement in the hydrophilic characteristics of the GO-incorporated membranes (the higher the hydrophilic characteristics of the membranes, the easier for the movement of water molecules through them) **He *et al.* (2015), Xia *et al.* (2015)** and **Shi *et al.* (2018).** Furthermore, the FO water flux increased with a decrease in the thickness of the PA AL of the GO-incorporated membrane. The membrane water flux decreased when the concentration of GONs increased drastically, which might be ascribed to the slight increase in the thickness of the active layer.

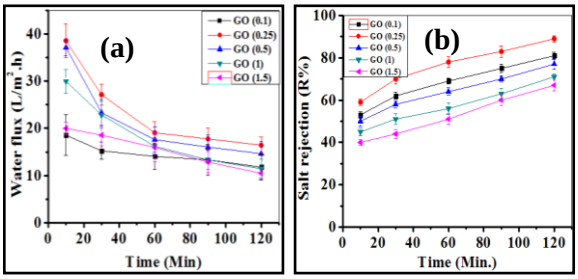

Fig. (7). (a) Pure water flux, (b) salt rejection of TFC employing different concentrations of GO from 0.1 to 1.5 wt%.

3.1.4. Effect of different concentration of dopamine

Figure (8) shows the different self-polymerizations of DA in the FO mode using DI water and 2 M of NaCl as the FS and DS, respectively. As shown in figure (8), 0.3 wt.% of DA is the ideal concentration for the reaction. The water flux increased to ~13.21 L/m^2.h, while the salt rejection reached 86%. Because a thin PA layer enhanced the hydrophilicity of the surface of the membrane, the water flux increased at a low degree of DA self-polymerization in the aqueous solution (**Wang *et al.* 2018**). However, as the DA self-polymerization increased significantly, the increases in the reverse solute flux of TFC Membranes were obvious when compared with the concentration in the current study. This phenomenon may be attributed to the PDA aggregation in high DA concentrations, which greatly hampered the interfacial polymerization process by the steric hindrance of PDA aggregations, leading to the intra-structure and low cross-linking surface with poor salt rejection.

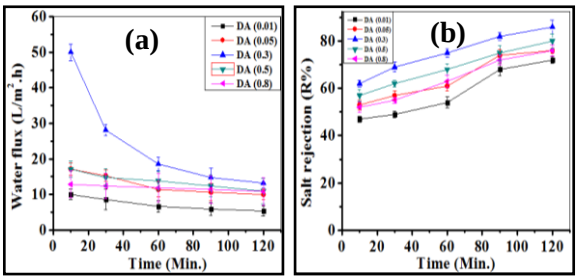

Fig. (8). (a) Pure water flux, (b) salt rejection of TFC employing different concentrations of DA from 0.01 to 0.8 wt%.

3.1.5 Effect of mix of GO, HA and DA membrane

Figure (9) shows the water fluxes of the FO membranes that were doped with a mixture of the optimum concentrations of GONs, HA, and DA. The comparison of the water fluxes of the HA, GO, DA, and mixed membranes showed that the mixed membrane achieved the best results. The water flux increased to ~33.21 L/m^2.h, while the salt rejection reached 98%. Improved hydrophilicity may be the cause of the further developed water transition through the combined HA, DA, and GO layer, which causes negatively charged responsive particles to collect on the film surfaces. After a period, the combined layer content accumulates, which in turn causes some film surface pores to get blocked and the combined film to agglomerate, causing water flux to decrease **(Xi 2009).** As a result, the film's porosity is high. Due to its high porosity and hydrophilicity, the mixed film was the best in this regard **(Xu *et al.* 2017).**

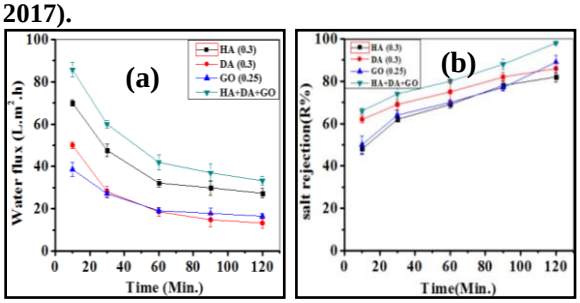

Fig. (9) (a) Pure water flux, (b) salt rejection of TFC employing GO, HA, DA, and mixed membranes.

3.2 Evaluation of the antiorganic fouling performance of the membrane

Figure (10) shows results of analyzing the membranes containing 0.3 wt.% of DA, 0.25 wt.% of GO, 0.3 wt.% of HA, and a mixture of DA, GO, HA/TFC doping. Here, Sodium Alginate (SA) was selected as the FS to examine the flux variations in the presence of 2 M of NaCl as the DS in the FO mode **Ang *et al.* (2011), Lee and Elimelech (2006)** and **Xie *et al.* (2017).**

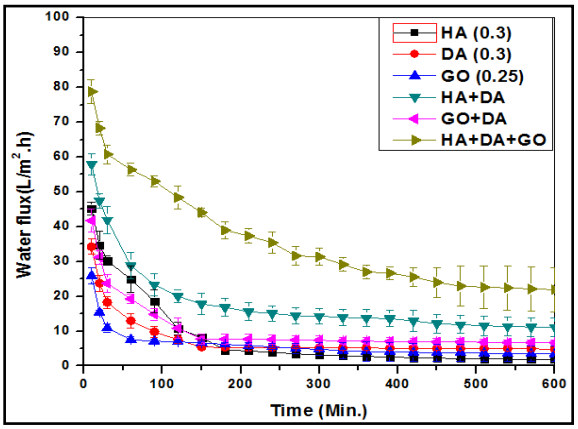

Fig. (10). Antifouling performance of the TFC-FO membrane that was modified with HA, DA, GO and a mix of HA, DA and GO.

The bridging and gel formation of SA by Ca^{2+} could explain the rapid decrease in the flow at the beginning. Furthermore, the initial strong permeation drag force contributed to the rapid decrease in the flux, resulting in a considerable hydraulic resistance and a rapid decrease in the flux. The gradual decrease

in the flux was observed after 300 min, indicating that the additional buildup of SA was insignificant. This result could be explained by the classical "critical flux concept." The result indicated that fouling would become insignificant once the critical flow was reached (**Tang *et al.* 2010**). At the conclusion of the fouling tests, the water flux of the mix HA, DA and GO-doped membranes showed a slower water flux decline ratio than that of the other membranes, showing a higher anti-organic fouling performance.

According to earlier research, a support layer that is more permeable would allow more water to pass through the membrane surface and result in a membrane surface that is less fouling propensity **Ramon and Hoek (2013).** Higher water permeability and a smoother surface were characteristics of the mix HA, DA and GO -modified support layer, which resulted in greater resistance to organic foulant. As a result, after changing the FO membrane with a mix of HA, DA and GO membranes, a higher anti-fouling performance could be achieved.

3.3 Chlorine resistance of the membrane

The chlorine resistance of the membrane was tested on the GO/TFC, HA/TFC, DA/TFC, and the mixture of GO, HA, and DA/TFC membranes **Fig. (11)**. The amide bonds of raw PA layers are sensitive to free chlorine and can be easily broken via *N*-chlorination, Orton rearrangement, and direct ring chlorination processes, which would increase the free volume of the PA layer as well as the flexibility of the polymer matrix. Thus, at the beginning of the degradation of the PA layer, it can be easily transferred by the water molecules; however, owing to the rapid degradation of the PA layer, low concentrations of GO, HA, and DA could reduce the degradation process of the PA layer when it is exposed to free chlorine, thereby exhibiting good chlorine resistance characteristics (75.0 times enhancement).

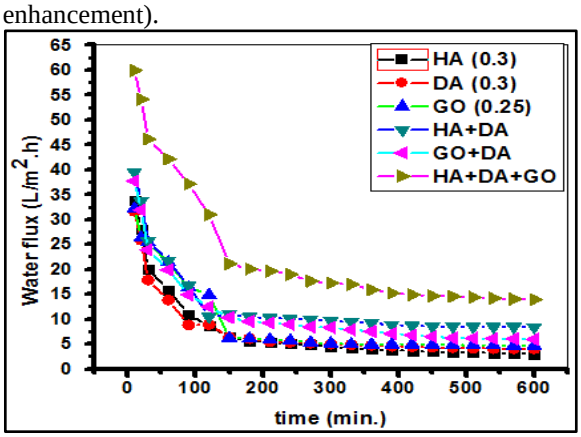

Fig. (11). Chlorine resistance performance of the TFC-FO membrane modified with HA, DA, GO and mix of HA, DA, GO.

Conclusion

Herein, we demonstrated that the porosity, structure, surface chemistry, and clean pure water flux of an FO membrane can be enhanced by incorporating a mixture of GO, HA and DA into its PES substrate. Moreover, additional COOH functional groups were introduced into the PA layer by embedding the layer with a mixture of GO, HA, and DA, making the surface more hydrophilic. Based on these results, the permeability–selectivity properties of the membrane can be improved. Further, the antifouling performance of this mixture-modified membrane was improved by the water flux. Furthermore, in terms of permeability and selectivity, the performance of this mixture-doped membrane could be compared with those of the commercial membranes. Thus, our results show that this mixture could be applied to the fabrication of cost-effective and efficient membranes.

Author Contributions

Dr/ Fatma Mohamed Elsayed: write the manuscript. Dr/ Abo Elfadl, dr/ abooly, dr/Heba Essawi and dr/ Mohamed, E.A.Ali are review the manuscript.

Conflicts of interest

The authors declare that they have no known competing financial interests or personal relationships that could have appeared to influence the work reported in this paper.

Acknowledgments

Deepest thanks for all the staff members & colleagues of Water & Soil Analysis Unit, Central Lab., Desert Research Centre for cooperation, giving access to the laboratory and research facilities.

Funding

There is no funding to report

4. References

Ali, M.E.; Wang, L.; Wang, X.; and Feng, X. (2016). Thin film composite membranes embedded with graphene oxide for water desalination. Desalination. 386: 67-76. doi: 10.1016/j.desal.2016.02.034.

Ang,W.S.; Tiraferri, A.; Chen, K.L. and Elimelech, M. (2011). Fouling and cleaning of RO membranes fouled by mixtures of organic foulants simulating wastewater effluent. J. Membr. Sci., 376: 196–206.

Cath, T.Y.; Amy, E.C. and Menachem, E. (2006). Forward Osmosis : Principles. Applications and Recent Developments. Ⅱ: 1–18.

Chang, X.; Wang, Z.; Quan, S.; Xu, Y.; Jiang, Z. and Shao, L. (2014). Exploring the synergetic effects of graphene oxide (GO) and polyvinylpyrrodione (PVP) on poly (vinylylidenefluoride) (PVDF) ultrafiltration membrane performance. Appl. Surf. Sci., 316:

537-548 .

Emadzadeh, D.; Lau, W.J.; Matsuura, T.; Hilal, N. and Ismail, A.F. (2014). The potential of thin film nanocomposite membrane in reducingorganic fouling in forward osmosis process. Desalination. 348: 82–88 .

Ghaseminezhad, S.M.; Barikani, M. and Salehirad, M. (2019). Development of graphene oxide-cellulose acetate nanocomposite reverse osmosis membrane for seawater desalination. Compos Part B Eng., 161: 320-327 .

Ghosh, A.K. and Hoek, E.M. (2009). Impacts of support membrane structure and chemistry on polyamide–polysulfone interfacial composite membranes. Journal of membrane science. 336(1-2): 140-148 .

Ghosh, A.K. and Hoek, E.M. (2009). Impacts of support membrane structure and chemistry on polyamide–polysulfone interfacial composite membranes. Journal of membrane science. 336(1-2): 140-148.

Guan, Y.F.; Chen, Q.; Wei, C.; Bao, C.H.; Yun, J.W. and Han, Q.Y. (2019). Modification of forward osmosis membrane with naturally available humic acid: Towards simultaneously improved filtration performance and antifouling properties. Environment International. 131: 1-8. doi: 10.1016/j.envint. 2019.105045.

Guan, Y.F.; Huang, B.C.; Qian, C.; Wang, L.F. and Yu, H.Q. (2017). Improved PVDF membrane performance by doping extracellular polymeric substances of activated sludge. Water Res., 113: 89–96 .

Han, G.; Zhang, S.; Li, X.; Widjojo, N. and Chung, T. (2012). Thin film compositeforward osmosis membranes based on polydopamine modified polysulfone substrates with enhancements in both water flux and salt rejection. Chem. Eng. Sci., 80: 219–231 .

He, L.; Dumée, L.F.; Feng, C.; Velleman, L.; Reis, R.; She, F. and et al. (2015). Promoted water transport across graphene oxide–poly (amide) thin film composite membranes and their antibacterial activity. Desalination. 365: 126–135. doi: 10.1016/j.desal.02.032.

Hirata, M.; Gotou, T.; Horiuchi, S.; Fujiwara, M. and Ohba, M. (2004). Thin-film particles of graphite oxide 1. Carbon. 42: 2929–2937. doi: 10.1016/j.carbon.2004.07.003.

Huang, G.; Kang, W.; Geng, Q.; Xing, B.; Liu, Q.; Jia, J. and Zhang, C. (2018). One-step green hydrothermal synthesis of few-layer graphene oxide from humic acid. Nanomaterials. 8: 1-9. doi: 10.3390/nano8040215.

Huang, H.; Mao, Y.; Ying, Y.; Liu, Y.; Sun, L. and Peng, X. (2013). Salt concentration, pH and pressure controlled separation of small molecules through lamellar graphene oxide membranes. Chem. Commun., 49: 5963–5965.

Huang, Y. et al. (2015). Synthesis and Characterization of a Polyamide Thin Film Composite Membrane Based on a Polydopamine Coated Support Layer for Forward Osmosis. RSC Advances. 128: 106113-106121.

Hummers, W.S. Jr. and Offeman, R.E. (1958). Preparation of graphitic oxide. J. Am. Chem. Soc., 80(6): 13-39. doi: 10.1021/ja01539a017.

Jing, G.G.; Xiao, L.G.; Wei, W.W.; Xin, Z. and Wu-Li, K. (2014). An ultrafast water transport forward osmosis membrane: porous grapheme. J. Mater. Chem. A., 2: 4023–4028 .

Khayet, M. and García, P.C.M. (2009). X-Ray diffraction study of polyethersulfone polymer, flat-sheet and hollow fibers prepared from the same under different gas-gaps. Desalination. 245: 494-500 .

Khorshidi, B.; Thundat, T.; Fleck, B.A. and Sadrzadeh, M. (2015). Thin film composite polyamide membranes: parametric study on the influence of synthesis conditions. RSC Advances. 5(68): 54985-54997.

Konch, T.J.; Gogoi, R.K.; Gogoi, A.; Saha, K.; Deka, J.; Reddy, K.A. and Raidongia, K. (2018). Nanofluidic transport through humic acid modified graphene oxide nanochannels. Mater. Chem. Front., 2: 1647–1654.

Kong, F.X.; Yang, H.W.; Wang, X.M. and Xie, Y.F. (2014). Rejection of nine haloacetic acids and coupled reverse draw solute permeation in forward osmosis. Desalination. 341: 1-9.

Lee, H.; Scherer, N.F. and Messersmith, P.B. (2006). Single-molecule mechanics of mussel adhesion. Proc. Natl. Acad. Sci., U.S.A. 103(35): 12999 –13003. doi: 10.1073/pnas.0605552103 .

Lerf, A.; He, H.Y.; Forster, M. and Klinowski, J. (1988). Structure of graphite oxide revisited. J. Phys. Chem., 102: 4477–4482.

Liu, Z. and Hu, Y. (2016). Sustainable antibiofouling properties of thinfilm composite forward osmosis membrane with rechargeable silver nanoparticles loading. ACS Appl. Mater. Interfaces. 8: 21666–21673 .

Lu, P.; Liang, S.; Zhou, T.; Mei, X.; Zhang, Y.; Zhang, C. and et al. (2016). Layered double hydroxide/graphene oxide hybrid incorporated polysulfone substrate for thinfilm nanocomposite forward osmosis membranes. RSC Adv., 6: 56599–56609. doi: 10.1039/c6ra10080e.

Lu, P.; Liu, Y.; Zhou, T.; Wang, Q. and Li, Y. (2018). Recent advancesin layered double hydroxides (LDHs) as two-dimensional membrane materials for gas and liquid separations. J Memb. Sci., 567: 89–103 .

Luo, H.; Gu, C.; Zheng, W.; Dai, F.; Wanga X. and Zheng. Z. (2015). Facile synthesis of novel size-controlled antibacterial hybrid spheres using silver nanoparticles loaded with poly-dopamine spheres. RSC Adv., 5: 13470–13477.

Ma, D.; Peh, S.B.; Han, G.; and Chen, S.B. (2017). Thin-film nanocomposite (TFN) membranes incorporated with super-hydrophilic metal–organic framework (MOF) UiO-66: toward enhancement of water flux and salt rejection. ACS Applied Materials & Interfaces. 9(8): 7523-7534.

Marcovecchio, M.G.; Mussati, S.F.; Aguirre, P.A. and Nicolás, J. (2005). Optimization of hybrid desalination processes including multi stage flash and reverse osmosis systems. Desalination. 182(1-3): 111-122.

Mazlan, N.M.; Peshev, D. and Livingston, A.G. (2016). Energy consumption for desalination—A comparison of forward osmosis with reverse osmosis, and the potential for perfect membranes. Desalination. 377: 138-151.

McCutcheon, J.R.; McGinnis, R.L. and Elimelech, M. (2005). A novel ammonia- carbon dioxide forward (direct) osmosis desalination process. Desalination. 174: 1-11.

Obaid, M.; Kang, Y.; Wang, S.; Yoon, M.H.; Kim, C.M.; Song, J.H. and Kim, I.S. (2018). Fabrication of highly permeable thin-film nanocomposite forward osmosis membranes via the design of novel freestanding robust nanofiber substrates. Journal of Materials Chemistry A. 6(25): 11700-11713.

Park, M.J.; Phuntsho, S.; He, T.; Nisola G.M.; Tijing, L.D. and Li, X.M. (2015). Graphene oxide incorporated polysulfone substrate for the fabricationof flat-sheet thinfilm composite forward osmosis membranes. J. Memb. Sci., 493: 496–507 .

Park, S. and Ruoff, R.S. (2009). Chemical methods for the production of graphenes. Nat. Nanotechnol. 4: 217 – 224. doi: 10.1038/nnano.2009.58 .

Ramon, G.Z. and Hoek, E.M. (2013). Transport through composite membranes, part 2: Impacts of roughness on permeability and fouling. Journal of membrane science. 425: 141-148.

Salehi, H.; Rastgar, M. and Shakeri, A. (2017). Anti-fouling and high water permeable forward osmosis membrane fabricated via layer by layer assembly of chitosan/graphene oxide. Applied Surface Science. 413: 99-108.

Santos, A.M.; Bertoli, A.C.; Borges, A.C.C.; Gomes, R.A.; Garcia, J.S. and Trevisan, M.G. (2018). New organomineral complex from humic substances extracted from poultry wastes: synthesis, characterization and controlled release study. Journal of the Brazilian chemical society. 29: 140-150.

Shaffer, D.L.; Werber, J.R.; Jaramillo, H.; Lin, S. and Elimelech, M. (2015). Forward osmosis: where are we now? Desalination. 356: 271-284.

She, Q.; Wong, Y.K.W.; Zhao, S. and Tang, C.Y. (2013). Organic fouling in pressure retarded osmosis: Experiments, mechanisms and implications. Journal of Membrane Science. 428: 181-189.

Shi, M.; Wang, Z.; Zhao, S.; Wang, J.; Zhang, P. and Cao, X. (2018). A novel pathway for high performance RO membrane: preparing active layer with decreased thickness and enhanced compactness by incorporating tannic acid into the support. J. Memb. Sci., 555: 157–168. doi: 10.1016/j.memsci.2018.03.025.

Siburian, R; Sihotang, H; Lumban, R.S.; Supeno, M. and Simanjuntak C. (2018). New route to synthesize of graphene nano sheets. Orient J. Chem., 34(1): 182-187. doi:10.13005/ojc/340120.

Singh, P.S.; Joshi, S.V.; Trivedi, J.J.; Devmurari, C.V.; Rao, A.P. and Ghosh, P.K. (2006). Probing the structural variations of thin film composite RO membranes obtained by coating polyamide over polysulfone membranes of different pore dimensions. Journal of membrane science. 278(1-2): 19-25.

Song, X.; Wang, L.; Mao, L. and Wang, Z. (2016). Nanocomposite membrane with different carbon nanotubes location for nanofiltration and forward osmosis applications. ACS Sustainable Chemistry & Engineering. 4(6): 2990-2997.

Szabó, T.; Szeri, A. and Dékány, I. (2005). Composite graphitic nanolayers prepared by self-assembly between finely dispersed graphite oxide and a cationic polymer. Carbon N. Y. 43: 87–94.

Tang, C.Y.; She, Q.; Lay, W.C.L.; Wang, R. and Fane, A.G. (2010). Coupled effects of internal concentration polarization and fouling on flux behavior of forward osmosis membranes during humic acid filtration. J. Membr. Sci., 354: 123–133 .

Wang, Y.; Fang, Z.; Xie, C.; Zhao, S.; Ng, D. and Xie, Z. (2018). Dopamine incorporated forward osmosis membranes with high structural stability and chlorine resistance. Processes. 6: 1–12. doi: 10.3390/pr6090151 .

Werber, J. R.; Deshmukh, A. and Elimelech, M. (2016). The critical need for increased selectivity not increased water permeability, for desalination membranes. Environmental Science & Technology Letters. 3(4): 112-120.

Widjojo, N.; Chung, T.S.; Weber, M.; Maletzko, C. and Warzelhan, V. (2013). A sulfonated polyphenylenesulfone (sPPSU) as the supporting substrate in thin film composite (TFC) membranes with enhanced performance for forward osmosis (FO). Chemical

engineering journal. 220: 15-23.

Xi, Z.Y. (2009). A facile method of surface modification for hydrophobic polymer membranes based on the adhesive behavior of poly (DOPA) and poly (dopamine). Journal of Membrane Science. 327(1-2): 244-253 .

Xia, S.; Yao L.; Zhao, Y.; Li, N. and Zheng, Y. (2015). Preparation of grapheme oxide modified polyamide thin film composite membranes with improved hydrophilicity for natural organic matter removal. Chem. Eng. J., 280: 720–727. doi: 10.1016/j.cej.06.063 .

Xie, Z.; Nagaraja, N.; Skillman, L.; Li, D. and Ho, G. (2017). Comparison of polysaccharide fouling in forward osmosis and reverse osmosis separations. Desalination. 402: 174–184 .

Xu, W.; Chen, Q. and Ge, Q. (2017). Recent advances in forward osmosis (FO) membrane: Chemical modifications on membranes for FO processes. Desalination. 419: 101-116 .

Zhao, D.; Chen, S.; Wang, P.; Zhao, Q. and Lu, X. (2014). A dendrimer-based forward osmosis draw solute for seawater desalination. Industrial & Engineering Chemistry Research. 53(42): 16170-16175.

Zhao, S.; Zou, L. and Mulcahy, D. (2012). Brackish water desalination by a hybrid forward osmosis–nanofiltration system using divalent draw solute. Desalination. 284: 175–181 .

Zhou, T.; Huang, S.; Niu, D.; Su, L.; Zhen, G. and Zhao, Y. (2018). Efficient separation of watersoluble humic acid using (3-aminopropyl) triethoxysilane (APTES) for carbon resource recovery from wastewater. ACS Sustain. Chem. Eng., 6: 5981–5989**.**